Kosterlitz-Thouless Transition for ^{4}He Films Adsorbed to Rough Surfaces

D. R. Luhman and R. B. Hallock

Laboratory of Low Temperature Physics, Department of Physics, University of Massachusetts, Amherst, Massachusetts 01003, USA

(Received 21 April 2004; published 19 August 2004)

We report the study of adsorption isotherms of ^{4}He on several well characterized rough CaF_2 surfaces using a quartz crystal microbalance technique at 1.672 K. The signature of decoupled mass observed on crossing the Kosterlitz-Thouless transition as a function of ^{4}He film thickness decreases and becomes increasingly difficult to identify as the surface roughness is increased. A peak in the dissipation, indicative of the onset of superfluidity, changes little with roughness.

DOI: 10.1103/PhysRevLett.93.086106 PACS numbers: 68.35.Ct, 64.70.Ja, 67.40.Pm, 68.15.+e

Thin ^{4}He films are known to exhibit superfluidity at sufficiently low temperatures. A hallmark of the static Kosterlitz-Thouless (KT) [1] theory is the discontinuous jump in superfluid density at the transition. Nelson and Kosterlitz [2] showed that the areal superfluid density σ_s at the transition temperature T_{KT} is given by the universal relation

$$\sigma_s = \frac{2m^2 k_B T_{\mathrm{KT}}}{\pi\hbar^2}, \tag{1}$$

where m is the mass of one helium atom. In practice, this discontinuity is rounded due to a finite frequency and flow velocity effects [3,4]. A number of experiments have confirmed predictions [1–4]: those utilizing torsional oscillators [5,6], quartz crystal microbalances (QCMs) [7], third sound [8] and thermal conductance [9,10] measurements. A peak in the dissipation near the KT transition related to the motion of vortices predicted by the dynamical theory [3], first observed by Bishop and Reppy [5], is another signature of the two-dimensional superfluid transition in thin helium films.

In torsional oscillator [6] experiments, the frequency of oscillation is directly related to the adsorbed mass seen by the substrate, and a shift in frequency is observed as the system is taken through the KT transition. Since actual substrates are not perfect, the observed frequency shift is typically not as would be expected for a perfect substrate. The mass that is observed to decouple from the substrate is related to $1 - \chi$, where χ is called the tortuosity factor. Generally, χ is fixed for a given experiment. In porous three-dimensional situations, the presence of superfluid is also documented by mass decoupling, and a tortuosity factor is used to account for geometric effects that influence the frequency shift [11].

In this Letter, we report a systematic QCM study of the observed frequency shift and dissipation at the KT transition as the surface roughness increases. By depositing CaF_2 of increasing nominal thicknesses on a series of QCMs, we are able to create a sequence of substrates with increasing surface roughness. As the surface roughness increases, the behavior of the observed frequency shift changes. A dissipation peak indicating the superfluid transition is seen on all samples. A previously reported QCM experiment with ^{4}He adsorption on CaF_2 films rougher than those used here did not resolve a frequency shift corresponding to the onset of superfluidity [12] but the dissipation was not measured. The presence of superfluidity on such rough surfaces was confirmed by third sound measurements [13] and hysteric adsorption was observed [12].

A series of seven gold-plated AT-cut QCM crystals with a fundamental resonance of 5 MHz [14] was used simultaneously in this experiment: six coated with CaF_2 and one uncoated (plain) crystal. The same amount of CaF_2 was thermally deposited on each side of a given crystal, and the entire area of each side was exposed during deposition. The CaF_2 was deposited at a rate of 0.2 nm/s and the nominal deposition thicknesses t for the series of QCMs ranged from 10 to 120 nm. The value of the CaF_2 coverage, t, for each sample was determined from the deposition observed on a separate QCM, measured simultaneously with the deposition on each QCM used in the ^{4}He adsorption measurements. t is reported here as a film thickness presuming the bulk density of CaF_2. The actual film thickness t_p is related to t through [15] $t_p = t/(1 - \phi)$, where ϕ is the three-dimensional porosity of the deposited CaF_2; $\phi \approx 0.64$.

The crystals were mounted vertically in a brass sample chamber and the assembly was inserted into a ^{4}He-pumped Dewar. The crystals were operated in the third harmonic (15 MHz) and the measured Q value of each was $Q \sim 8 \times 10^4$ at the operating temperature of $T = 1.672$ K. The sensitivity of the QCMs operated in this mode is 1.77 Hz/layer, where an atomic layer of adsorbed ^{4}He is defined as 0.36 nm. The frequency of the QCMs was measured using a dc frequency modulated feedback technique [16]. This technique minimizes noise and allows for the measurement of the dissipation ($\sim Q^{-1}$). For high Q oscillators the amplitude of oscillation at resonance is expected to be proportional to Q, and thus Q can be monitored. The drive voltage applied to the QCMs was 400 μV, and as a result the vibration ampli-

 © 2004 The American Physical Society

tude of the crystals was quite small and is estimated to be 5 pm [17]. Similar results were seen for 800 μV and no heating effects were observed.

^{4}He was incrementally added to the cell, and frequency and dissipation data were collected for each crystal after each addition. The Dewar bath pressure P_0 and the pressure in the sample cell, P, were measured for each data point. Figure 1 shows the adsorption isotherm for each of the QCMs as a function of P/P_0 at $T = 1.672$ K. We have defined $\Delta f = f - f_r$, where f is the frequency measured for each value of P/P_0 and f_r is the frequency measured with no ^{4}He in the sample chamber. $-\Delta f$ is directly proportional to the amount of ^{4}He coupled to the surface of a particular QCM. For larger values of t the amount of helium adsorption increases due to the additional roughness of the surface, which increases the surface area and may provide pockets for capillary condensation. Desorption data were also collected on the crystals but had considerable noise, particularly for the lower t crystals. The Δf desorption data on the $t = 60$ nm and $t = 120$ nm crystals were sufficient to observe hysteresis loops suggesting capillary condensation. The noise in the desorption data for the remainder of the QCMs precluded the observation of any hysteresis loops. An additional QCM was used with $t = 90$ nm, but due to technical problems only first harmonic dissipation data were available. Near $P/P_0 = 0.68$ there is a visible signature in the data, which is associated with the superfluid transition. For larger t the relative distinctness of the feature decreases. For $t = 120$ nm the feature is not readily visible, although near $P/P_0 = 0.68$ there is a very subtle shift in the slope of the isotherm, which may be due to the onset of superfluidity.

Figure 2 shows both Δf and Q^{-1} data for the transition region for all crystals, including the dissipation for $t = 90$ nm. To better display the features relevant to the KT transition, we have plotted the data versus ^{4}He film thickness on glass, d_g, which we determined using the approximate relation $d_g^3 = \alpha/[T \ln(P_0/P)]$, where α is the van der Waals constant; $\alpha = 27$ (layers)^3 K for ^{4}He on glass. The data in the figure are offset vertically for clarity. The shift in Δf for $3.4 < d_g < 4.2$ layers is due to the superfluid transition. In addition, the peak in Q^{-1} persists even to the largest values of t, indicating the onset of superfluidity. If we use the size of the trough to peak frequency shift on the plain QCM in Fig. 2 as an estimate for the superfluid decoupling at the transition, we obtain $\sigma_s = 5.0 \pm 0.5$ ng/cm^2, modestly close to $\sigma_s = 5.85$ ng/cm^2 predicted from Eq. (1).

To more readily observe and quantitatively compare the frequency shift between different QCMs, we must take into account the increase in slope of the isotherms near the transition. When the entire isotherm is plotted versus d_g, a linear region on the thin film side of the KT transition is visible. The data on the thick film side of the transition in Fig. 2 are also fairly linear in each case. Therefore, we define the transition region to span from the end of the linear region for small d_g to the start of the

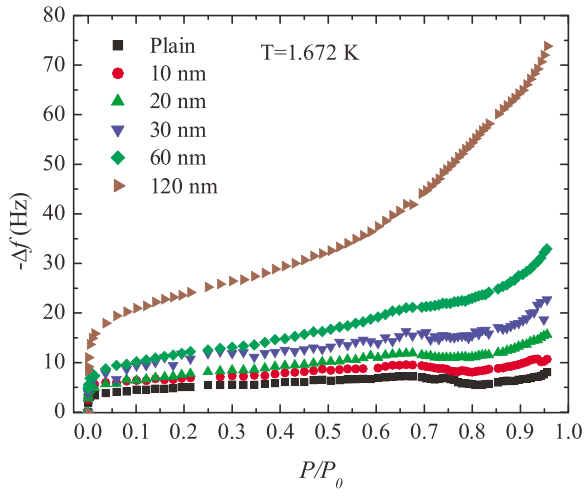

FIG. 1 (color online). Adsorption isotherm for each of the QCMs. The feature in the data near $P/P_0 = 0.68$ is the KT transition (see Fig. 2). The numbers in the legend correspond to the nominal film thickness t of the CaF_2.

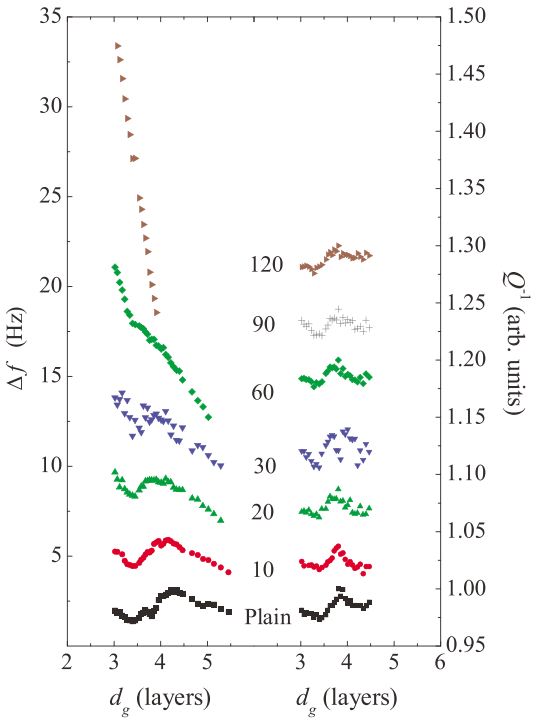

FIG. 2 (color online). Δf and Q^{-1} versus d_g for all QCMs. The vertical row of numbers in the center of the plot corresponds to the nominal thickness of the CaF_2 film t in nanometers. The data have been offset by a constant for clarity, and therefore the vertical scale axes are provided for relative comparison of the KT transition related features. We have also included first harmonic Q^{-1} data for the $t = 90$ nm sample where meaningful frequency data was not attainable. The small feature in Δf near $d_g = 3.75$ layers on the plain crystal is due to noise.

linear region for large d_g. For small t, this definition roughly coincides with the region between the dip and the peak of the Δf data in Fig. 2. A line best fit to the linear region for small d_g for each data set was subtracted from the data. The results of the subtraction near the transition for the $t = 0$, 20, and 60 nm data are shown in Figs. 3(a)–3(c). Plots such as these reveal a frequency shift that changes character and becomes less well defined for increasing values of t. Our primary conclusion is that the frequency shift seen on increasingly rough (disordered) surfaces becomes less and less identifiable with the frequency shift anticipated based on Eq. (1), but the Kosterlitz-Thouless transition is present as indicated by the presence of the dissipation peak, Fig. 2. At the transition there is 3 times more ^{4}He adsorbed on the $t =$ 60 nm substrate compared to the plain QCM. This additional mass does not contribute to the frequency shift, presumably due to tortuosity.

Using the above definition of the transition region, an observed frequency shift δ can be somewhat arbitrarily defined [18] as the change in frequency across the transition in the subtracted data Δ. The resulting δ are shown in Fig. 3(d), showing a decrease in δ as t increases. If we use the value of δ found on the plain QCM, δ_g, as the expected frequency shift for a nonrough substrate, we can define a measured value for the relative effect of the changing disorder as δ/δ_g. If, in addition, we assume that disorder and tortuosity are related and define $1 - \chi = \delta/\delta_g$, we find values for χ that are consistent with those found from third sound index of refraction, n, data [13] when the third sound and QCM surfaces have similar roughness if the connection [19] $n^2 = (1 - \chi)^{-1}$ is used. We emphasize that the presence of increasing roughness makes a clear determination of the frequency shift difficult. In Fig. 3(e) we have plotted the value of d_g where the KT transition occurs, d_{KT}, as determined by the position of the peak in the dissipation and find that it does not change with an increase in roughness.

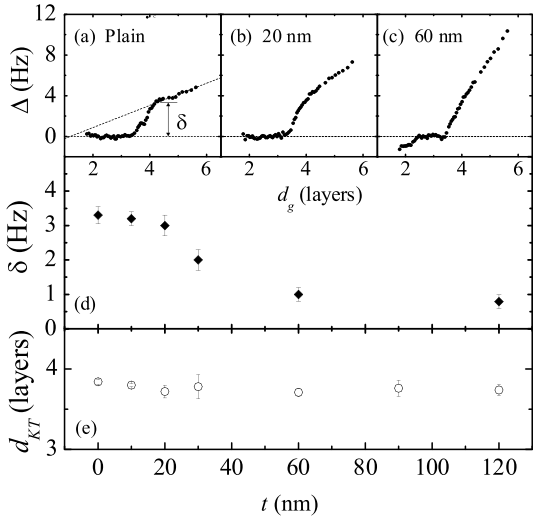

FIG. 3. Examples of the data for the frequency shift Δ, as described in the text for $t =$ (a) 0, (b) 20, and (c) 60 nm. (d) δ vs t. (e) d_{KT} vs t. d_{KT} is the value of d_g at the KT transition as determined by the peak in Q^{-1}.

To further characterize our surfaces, we used atomic force microscopy (AFM) to image the surfaces of the QCMs directly [20]. The CaF_2 surface atop the gold electrodes was imaged to produce 512×512 pixel images of an area 1 μm $\times$ 1 μm in size. The height distribution of each image was well fit by a Gaussian function of width σ_z. The value of σ_z was taken as a typical length scale of the surface structure perpendicular to the substrate. To obtain a quantitative measure for the lateral surface structure, we fit the results of a two-dimensional correlation calculation of the image to a bivariate Gaussian distribution with width σ_{xy}. A more detailed description of these surface characterization calculations is presented elsewhere, along with a thorough analysis of a range of CaF_2 films on glass [15]. σ_z and σ_{xy} averaged from several images for each value of t are shown as the solid symbols in Fig. 4. σ_z shows an increasing trend with t. σ_{xy} shows a similar trend generally consistent with what was seen for CaF_2 deposited on glass [15]. These parameters provide direct evidence for the increase in surface roughness of the CaF_2 films, which in turn causes the changes in the observed frequency shift shown in Figs. 3(a)–3(d).

We are not able to directly measure the actual thickness of the CaF_2 films on the QCMs using profilometer measurements because the entire surface is covered with CaF_2, resulting in no uncovered area where t_p can be measured. As a result, we cannot measure the porosity ϕ of the CaF_2 films on the QCMs directly. Instead, to obtain an estimate for ϕ on the QCMs, we deposited CaF_2 with the same values of t onto regions of the surface on a series of glass substrates coated with a thin film of gold. The porosity of these films was found to be constant over the entire range of t studied and was determined to be $\phi = 0.64 \pm 0.01$. The values of σ_z and σ_{xy} for these

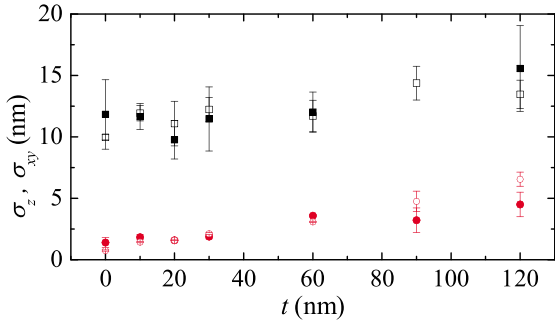

FIG. 4 (color online). The surface characterization parameters σ_z (circles) and σ_{xy} (squares) versus t. The solid symbols correspond to the QCMs, while the open symbols correspond to CaF_2 deposited on gold-plated glass substrates. The $t = 0$ nm points represent the gold surfaces with no CaF_2 deposited.

coated glass substrates are shown in Fig. 4 as open symbols [21]. The surface parameters are in good agreement with those found from the QCMs and as a result we use $\phi = 0.64 \pm 0.01$ as an estimate for the porosity of the CaF_2 films deposited on the QCMs.

The AFM images reveal that the surface structure of the CaF_2 films consists primarily of a collection of closely spaced raised structures [22]. Between the raised structures, pores are created that are able to trap fluid due to capillary condensation. The larger the structures, i.e., the rougher the CaF_2, the more fluid is trapped in these interstitial regions. This is evident by comparing the increasing trend seen in σ_z (Fig. 4) with the increase in adsorption as t increases as shown Fig. 1. It is also interesting to note that, even though approximately 6 times more ^{4}He is adsorbed to the $t = 120$ nm substrate than the plain QCM near the KT transition, there is little or no change in d_{KT}.

Recent preliminary numerical calculations have shown that the tortuosity χ is a function of the porosity and not of the pore size for a three-dimensionally connected porous substrate [23]. Our experiments do not address this directly. Our data show that as the surface roughness and surface pore size increase with constant porosity we see a decrease in the observed frequency shift. We cannot unambiguously establish whether or not there may be a porous interior connected to the surface.

In conclusion, we have studied the change in behavior of the QCM frequency shift at the KT transition as the surface roughness of the substrate is systematically increased. We find that the roughness introduces substantial changes in the character of the frequency shift [24] with little or no change in the dissipation or the location of the Kosterlitz-Thouless transition in the film thickness-temperature phase diagram.

We thank K. J. Thompson for assistance and J. Machta and N. Prokof'ev for stimulating discussions. This work was supported by the National Science Foundation under Grants No. DMR-0138009 and No. DMR-0213695 (MRSEC) and also by research trust funds administered by the University of Massachusetts Amherst.

[1] J. M. Kosterlitz and D. J. Thouless, J. Phys. C **6**, 1181 (1973).
[2] D. R. Nelson and J. M. Kosterlitz, Phys. Rev. Lett. **39**, 1201 (1977).
[3] V. Ambegaokar, B. I. Halperin, D. R. Nelson, and E. Siggia, Phys. Rev. B **21**, 1806 (1980).
[4] B. A. Huberman, R. J. Myerson, and S. Doniach, Phys. Rev. Lett. **40**, 780 (1978).
[5] D. J. Bishop and J. D. Reppy, Phys. Rev. Lett. **40**, 1727 (1977); Phys. Rev. B **22**, 5171 (1980).
[6] G. Agnolet, D. F. McQueeney, and J. D. Reppy, Phys. Rev. B **39**, 8934 (1989); P. A. Crowell and J. D. Reppy, Phys. Rev. B **53**, 2701 (1996).
[7] M. Chester and L. C. Yang, Phys. Rev. Lett. **31**, 1377 (1973).
[8] I. Rudnick, Phys. Rev. Lett. **40**, 1454 (1978).
[9] J. Maps and R. B. Hallock, Phys. Rev. Lett. **47**, 1533 (1981); Phys. Rev. B **26**, 3979 (1982).
[10] G. Agnolet, S. L. Teitel, and J. D. Reppy, Phys. Rev. Lett. **47**, 1537 (1981).
[11] J. B. Mehl and W. Zimmermann, Jr., Phys. Rev. **167**, 214 (1968); G. K. S. Wong, P. A. Crowell, H. A. Cho, and J. D. Reppy, Phys. Rev. B **48**, 3858 (1993).
[12] J. C. Herrmann and R. B. Hallock, Phys. Rev. B **68**, 224510 (2003).
[13] See also D. Luhman and R. B. Hallock, Bull. Am. Phys. Soc. **49**, 166 (2004); J. Low Temp. Phys. (to be published).
[14] Colorado Crystal Corporation, 2303 8th Street, Loveland, Colorado 80537.
[15] D. R. Luhman and R. B. Hallock, Phys. Rev. E (to be published).
[16] M. J. Lea, P. Fozooni, and P. W. Retz, J. Low Temp. Phys. **54**, 303 (1984).
[17] See, e.g., B. Borovsky, B. L. Mason, and J. Krim, J. Appl. Phys. **88**, 4017 (2000); L. Bruschi, A. Carlin, and G. Mistura, Phys. Rev. Lett. **88**, 046105 (2002).
[18] Because of the finite width of the transitions, the frequency shifts δ are magnified compared to Fig. 2. We have analyzed the data using several other different definitions of δ, and in each case the fundamental result of δ decreasing as t, or roughness, increases remains unchanged. The ratios of the slope for large d_g to the slope for small d_g fluctuate a bit with t, but the interpretation of this ratio is complicated by capillary condensation.
[19] D. J. Bergman, B. I. Halperin, and P. C. Hohenberg, Phys. Rev. B **11**, 4253 (1975).
[20] The AFM tip radius (<10 nm) limits the resolution.
[21] The value of σ_{xy} for $t = 90$ nm on the gold-plated glass substrate was anomalous and is omitted.
[22] The images of the low nonzero t QCMs show a relatively small number of longer length scale lateral structures. We assume that the adsorption behavior is dominated by the small surface structure which covers the majority of the surface. This assumption is verified by Fig. 2.
[23] T. Obata, J. D. Reppy, and M. Kubota, J. Low Temp. Phys. **134**, 547 (2004).
[24] Recent experiments that utilize a QCM with porous gold electrodes of fixed porosity and pore size report no observable frequency shift near the observed dissipation peak; R. J. Lazarowich, P. Taborek, and J. E. Rutledge, Bull. Am. Phys. Soc. **49**, 378 (2004).